



## Computational fluid dynamic simulation of an inter-phasing pulse tube cooler<sup>\*</sup>

Xiao-bin ZHANG<sup>†1</sup>, Zhi-hua GAN<sup>†‡1</sup>, Li-min QIU<sup>1</sup>, Hua-xiang LIU<sup>2</sup>

(<sup>1</sup>Institute of Refrigeration and Cryogenics, Zhejiang University, Hangzhou 310027, China)

(<sup>2</sup>College of Science, Guangdong Ocean University, Zhanjiang 524088, China)

<sup>†</sup>E-mail: zhangxbn@zju.edu.cn; Gan\_zhuhua@zjuem.zju.edu.cn

Received May 21, 2007; revision accepted July 3, 2007; published online Dec. 8, 2007

**Abstract:** An inter-phasing pulse tube cooler (IPPTC) consists of two pulse tube units, which are connected to each other at hot ends of the pulse tubes through a needle valve. This paper presents the computational fluid dynamic (CFD) results of an IPPTC using a 2D axis-symmetrical model. General results such as the phase difference between pressure and velocity at cold end and hot end, the temperature profiles along the wall, the available lowest temperature as well as its oscillations and the coefficient of performance (COP) for IPPTC are presented. The formation of DC flow and its effects on the performance of the cooler are investigated and analyzed in detail. Turbulence, which is partially responsible for the poor overall performance of a single orifice pulse tube cooler (OPTC), is found to be much reduced in IPPTC and its performance is improved significantly compared with the single OPTC.

**Key words:** Inner-phasing, Pulse tube cooler (PTC), Computational fluid dynamic (CFD)

**doi:**10.1631/jzus.A071259

**Document code:** A

**CLC number:** TB651

### INTRODUCTION

Several phase-adjusting methods for the pulse tube cooler (PTC), such as double-inlet (Zhu *et al.*, 1990), four valves (Kaiser *et al.*, 1996) and inertance tube (Gardner and Swift, 1997), have been invented to improve the performance since the invention of the simple orifice pulse tube cooler (OPTC) in 1980s (Mikulin *et al.*, 1985). The inter-phasing pulse tube cooler (IPPTC), first proposed by Gao and Matsubara (1996), has better cooling capacity and coefficient of performance (COP) compared with its original counterparts, double-inlet and OPTC (Tanida *et al.*, 1997). The IPPTC (Fig.1) comprises of two pulse tube units and each unit has a regenerator and a pulse tube. The two units are linked through a needle valve

at hot ends of the pulse tubes, thus the reservoir is canceled. A double-outlet rotary valve together with the compressor unit supplies the oscillating pressure waves for the two units with a phasing difference. As a promising new type of PTC, the mechanism of phase-adjusting and the presence of unsteady thermodynamical processes have not been investigated. The present authors have analyzed the IPPTC using a 1D linear theory, and found a smaller phase difference between the velocity and the pressure at cold end compared with the double-inlet and simple orifice (Zhang and Qiu, 2005). However, the fluid in the pulse tube experiences a complex multi-dimensional flow process of mass and heat transfer, which has significant influence on the cooler. Consequently, the 1D model is insufficient to reveal the real gas flow characteristics in the pulse tube. This paper continues our previous computational fluid dynamic (CFD) modeling of an OPTC (Zhang *et al.*, 2007) to an IPPTC using the commercially available CFD code, Fluent.

<sup>‡</sup> Corresponding author

<sup>\*</sup> Project supported by the National Natural Science foundation of China (No. 50706042), the Science and Technology Department of Zhejiang Province (No. 2006C24G2010027) and the Natural Science Foundation of Zhejiang Province (No. Y105519), China

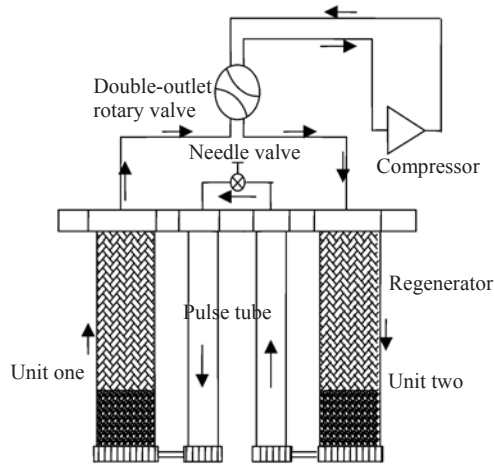


Fig.1 Schematic of inter-phasing pulse tube cooler

## PHYSICAL MODEL

The simulation model (Fig.2) is made up of two completely identical pulse tube units, which are linearly aligned and connected at the pulse tube hot ends through a needle valve (I). The two units are symmetrical about the needle valve and Fig.2 only shows one of them. Each unit comprises a regenerator (B) with an aftercooler (A), a pulse tube (E) with cold-end and hot-end heat exchangers (HXs) (D, F), transitional tubes (C, G) and a connecting tube (H). The aftercooler, the hot-end and cold-end HXs are modeled as porous regions filled with a copper matrix with a porosity of 0.697. The regenerator is also a porous region filled with a stainless steel wire matrix with a porosity of 0.694. Table 1 lists the operational parameters of the porous regions used in our CFD simulation. The model's geometries, mathematical

formulation and setup processes are the same as the case of the OPTC (Zhang *et al.*, 2007). Two sinusoidal oscillating pressure waves with 180° out of phase, described as Eqs.(1)~(2), are input to unit one and unit two, respectively:

$$p_1 = p_0 + \Delta p \sin(2\pi ft), \quad (1)$$

$$p_2 = p_0 - \Delta p \sin(2\pi ft), \quad (2)$$

where, time-averaged pressure  $p_0$  is 1.31 Mpa, pressure amplitude  $\Delta p$  is 0.375 MPa and frequent  $f$  is 1.5 Hz. The valve is modeled as a flow restriction where pressure drop is proportional to local area-averaged velocity (de Waele *et al.*, 1998; de Boer, 2000):

$$\Delta p' = -C_v \bar{v}. \quad (3)$$

The valve has a “ $C_v$ ” factor of 36000, which is set to twice the optimized value used in OPTC, since the pressure difference between two sides of the needle valve of the IPPTC is about twice larger than that of the OPTC (Zhang *et al.*, 2007).

## RESULTS AND ANALYSIS

Fig.3 shows the phase relationships between the pressure, the area-averaged axial velocity at cold end and the input pressure for unit one when there is no thermal load. It is found that the velocity is ahead of the pressure at cold end by about 50°, and the pressure at cold end lags behind the input pressure by about 8°, the corresponding values are 60° and 13° respectively for the OPTC (Zhang *et al.*, 2007).

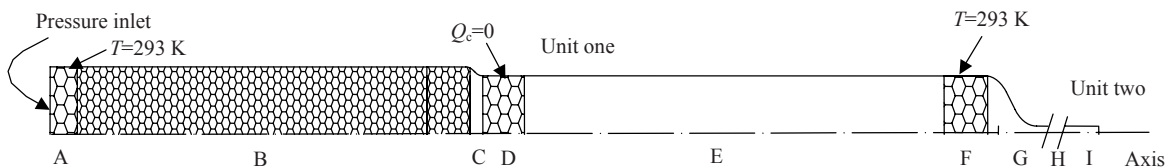


Fig.2 Simulation model of an inter-phasing pulse tube cooler. Unit two is a mirror image of unit one

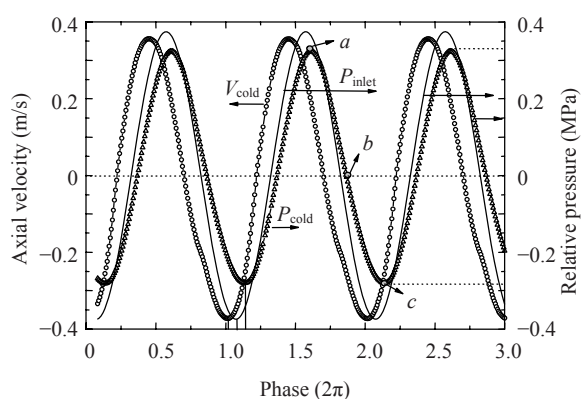
Table 1 Operational parameters of the porous media

Components	Material	$m$	$n$ ( $m^{-1}$ )	$d_w$ (m)	$l$ (m)	$\beta$	$\varepsilon$	$D$	$C_2$
Regenerator	304 S.S	247	$1.2 \times 10^4$	$4 \times 10^{-5}$	$6.3 \times 10^{-5}$	0.373	0.694	$5.95 \times 10^9$	$1.299 \times 10^4$
HXs	Copper	98	$1.0 \times 10^4$	$1 \times 10^{-4}$	$1.6 \times 10^{-4}$	0.377	0.697	$1.94 \times 10^9$	$1.15 \times 10^4$

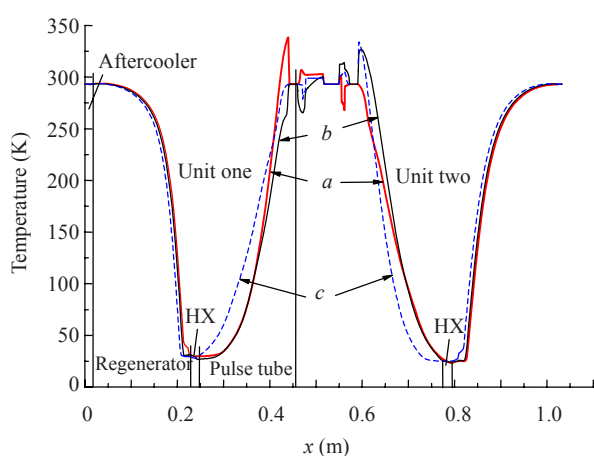
$m$ : mesh per inch;  $n$ : number of packed screens per length;  $d_w$ : wire diameter of screen;  $l$ : mesh distance;  $\beta$ : opening area ratio of screen;  $\varepsilon$ : porosity;  $D=1/\alpha$ ,  $\alpha$  is the permeability;  $C_2$ : inertial resistance factor

Fig.4 shows the temperature profiles along the walls of the whole cooler when the pressures are at points *a*, *b*, *c* in Fig.3. The temperature profiles are approximately symmetrical about the needle valve at the same moment, and similar to that of the OPTC (Zhang *et al.*, 2007), have the following features: (1) the temperature of the regenerator wall varies little in a cycle, especially for the hot region; (2) the temperature distribution along the wall of the pulse tube is not linear, changing gently at cold end and quickly at hot end. However, compared with the results of the OPTC, the curves for IPPTC are smoother because there is no turbulence in the pulse tube. A small region of almost constant temperature only appears at the regenerator side of the cold-end HX. The reason for the turbulence disappearance will be explained later in this paper.

DC flow is introduced into the IPPTC, because



**Fig.3 Pressure and velocity at cold end and input pressure as function of phase**



**Fig.4 Temperature profiles along the wall when the pressure is at points *a*, *b*, *c* in Fig.3**

the gas flow through the two regenerators undergoes different resistance processes in a cycle. Starting with the IPPTC at 273 K, as Eqs.(1) and (2) described, the gas in unit one is first compressed to over the time-averaged pressure in the first half of the first cycle, and the temperature increases. Simultaneously, the gas in unit two is first expanded below the time-averaged pressure, and the temperature decreases. The opposite is true in the second half of the first cycle (Fig.5). The gas in the two units does not experience a identical temperature cycle, therefore, it suffers different resistance processes in the respective regenerator for the temperature dependent viscosity, and thus forms the imbalanced time-averaged pressures. It is found from Fig.6 that the time-averaged pressure difference still exists when the cooler gets to its lowest temperature, which is about 2160 Pa higher in unit two than that in unit one, leading to a DC flow from unit two to unit one, as shown in Fig.1. By integrating the mass flow rate through the needle valve for several cycles, the value of the DC flow is found to be about  $-0.0367$  g in a cycle (the minus means the direction is from unit two to unit one). The value of the DC flow is about 1% of the total mass flow (3.63 g) at the inlet of unit one in a half of the first cycle, and the ratio increases a little when the loads at every cold end of the IPPTC are increased to 28 W.

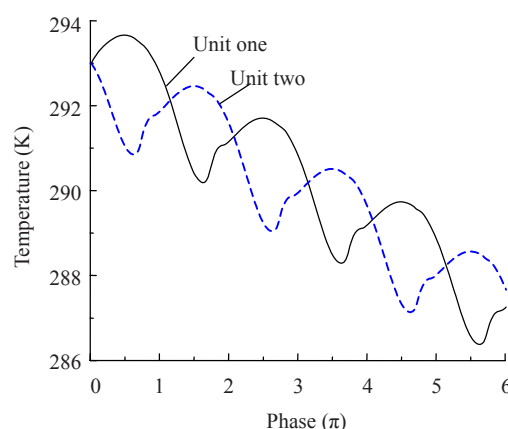


**Fig.5 Temperature at cold-end HXs varies as phase at beginning of simulation from 273 K**

The DC flow has a complex effect on the cooler. Wang *et al.*(1998a) calculated that a small mass ratio of DC flow to the AC flow, in any direction, will increase the cooling capacity for a single-stage double-inlet pulse tube cooler with the cold-end

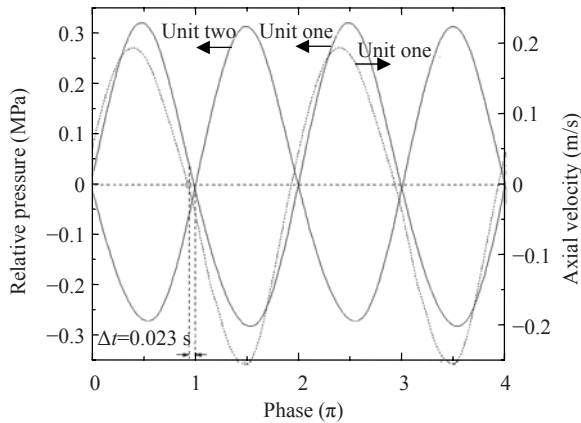


**Fig.6 Pressures in the two pulse tubes and velocity at hot end of unit one vs phase**

temperature of about 30 K. According to our simulation, the reason is that there is a small region of almost constant temperature at both sides of the cold-end HXs with a relatively low temperature. A small mass of DC flow, regardless of its direction, will always increase the cooling capacity. However, as the cold-end temperature drops below 30 K, the constant-temperature region having lower temperature in the pulse tube side can disappear, as shown in Fig.4, hence, a small mass of DC flow from the pulse tube will deteriorate the cooler. However, it seems that if the constant temperature region in the regenerator still exists, then, a small mass of DC flow from the regenerator will still benefit the cooler. The same phenomenon was also numerically and experimentally verified by Wang *et al.*(1998b) when the cold-end temperature is 4 K. As the DC flow is from unit two to unit one, it lowers the cold-end temperature of unit two and increases the cold-end temperature of unit one. It is found that the cold-end temperature of unit two is lower by about 4.9 K than that of unit one when there are no thermal loads, and the temperature difference increases to 5 K for the case of both 28 W loads because of the increase of the DC flow, accompanied by a decrease in the amplitude of temperature fluctuation from 1.25 K to 1 K, as shown in Fig.7.

Fig.8 shows the relationship between the cooling capacities and the cold-end temperature for IPPTC. The relationship for the OPTC is also plotted. The temperature for the two units goes up slowly when the load is small and quickly when the load becomes relatively large. The cooling capacities of unit two are always greater than unit one as a result of the DC

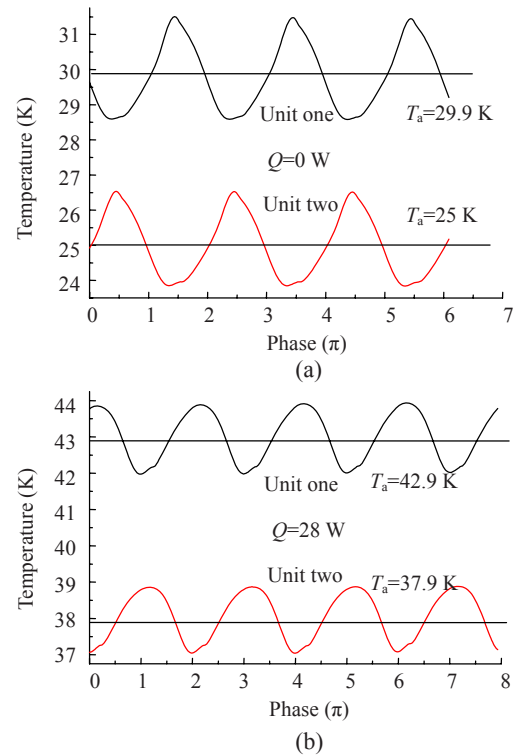


**Fig.7 Temperatures at two cold-end HXs as function of time on steady state**

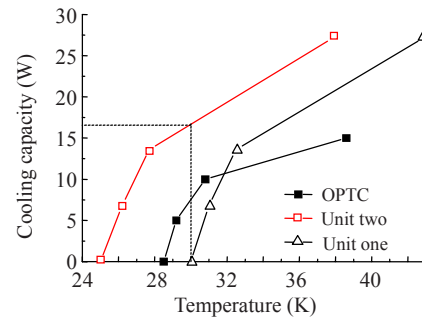


**Fig.8 Cooling capacity as function of temperature at cold end for the two units and the OPTC with different thermal loads**

flow, which can be validated by a simple calculation. Supposing the temperature  $T$  at both cold-ends is 30 K, substituting the value of DC flow  $m_{DC} = -0.0367$  g, the cycle  $\tau = 2/3$  s and the specific heat at constant pressure  $C_p = 5200$  J/kg into  $H_{DC} = m_{DC} C_p T / \tau$ , leads to  $H_{DC} \approx -8.59$  W. The result implies that 8.59 W enthalpy flow is transferred by the DC flow from unit two to unit one, leading to a difference of the cooling capacity of  $8.59 \times 2 = 17.18$  W, which is very close to the value of 16.8 W at 30 K in Fig.8. The cooling

capacity of the OPTC lies between the two units when the load is small, and becomes smaller than either of them as the load increases. The average of the cooling capacities of the two units is always greater than the OPTC, which accords well with experiment results (Gao and Matsubara, 1996; Tanida *et al.*, 1997).

Fig.9 shows the input  $P$ - $V$  work of the two units and the OPTC. The two units have reversed  $P$ - $V$  profiles for the opposite velocity direction. Due to turbulence, the curves for the OPTC are not as smooth as those for IPPTC. Unit two consumes a little more  $P$ - $V$  work than unit one due to the DC flow, however, the OPTC consumes much more  $P$ - $V$  work than unit one (the area enclosed by curves for OPTC is much larger than that for unit one). The average input work for the two units is smaller than that for the OPTC, and so the

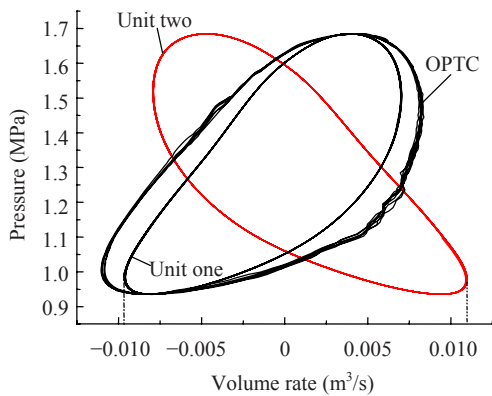


**Fig.9** Input  $P$ - $V$  work for the two units and the OPTC when there is no thermal load

COP of the IPPTC is higher than the OPTC.

Fig.10 shows the no-load temperature contours in the pulse tube of unit one when the pressures are at points  $a$ ,  $b$ ,  $c$  in Fig.3. The isotherms become more and more distorted as the pressure in the pulse tube expands from the highest to the lowest. However, unlike the OPTC, there is no swirl flow formed and the gas presents a desired axial temperature gradient. Our previous research (Zhang *et al.*, 2007) pointed out that in order to form a swirling flow pattern in the pulse tube, two preconditions must be met: (1) the boundary layer is adequately deep; (2) the relaxing time is long enough. The IPPTC has similar boundary layer distribution to the OPTC, however, it has much smaller relaxing time of 0.023 s ( $12.4^\circ$  out of phase, see Fig.6) than 0.032 s of the OPTC ( $17.3^\circ$  out of phase). It seems that 0.023 s does not meet the second precondition so that the swirling flow is restricted. The depth of the boundary layer in the pulse tube in Fig.10 accords well with the calculating results from the equation of  $\delta_k \approx \delta_v = \sqrt{2\mu/\omega\rho}$  (Olson and Swift, 1997). Olson and Swift pointed out that the gas elements in the boundary layer will experience a small net drift to the hot end in a cycle and thus form the streaming, which turns to the center in the vicinity of the hot HX and returns to the cold end along the center. Obviously, the circulatory flow of the streaming will lead to a higher temperature near the center than the interior at the same cross section, just as our simulation shown in Fig.10 revealed.

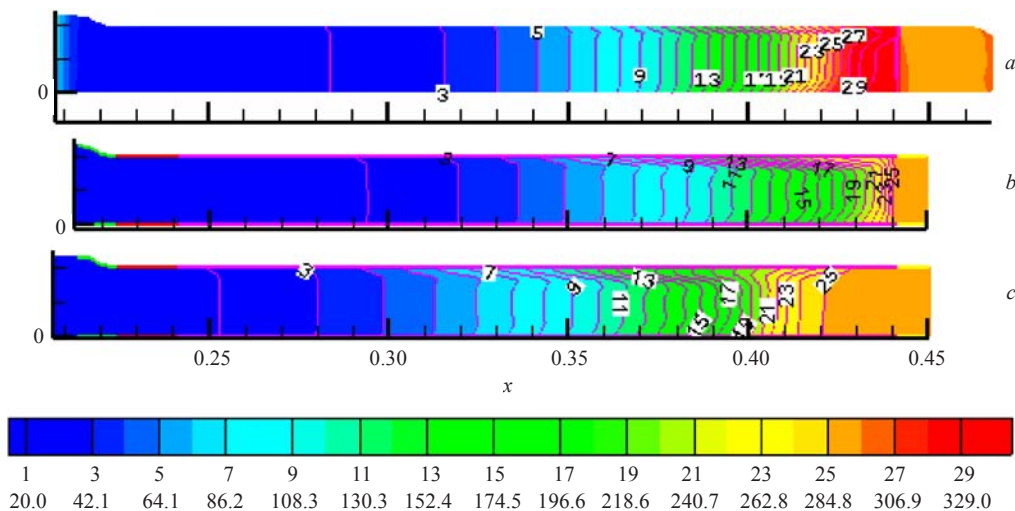


**Fig.10** Temperature contours of pulse tube when pressure is at points  $a$ ,  $b$ ,  $c$  in Fig.3

## CONCLUSION

An axis-symmetrical numerical simulation model for an IPPTC is developed, which has successfully predicted some multi-dimensional flow and thermo-dynamical characters in the pulse tube through solving the Navier-Stokes equations. The conclusions from our simulations are:

(1) Compared with the OPTC, the IPPTC has preferable phase relationship between the pressure and the velocity at hot end and cold end of the pulse tube.

(2) Although the two units have the same geometries and boundary conditions, they have different performances because of the DC flow. The direction of the DC flow determined by the start status of the input pressure, is from one unit expanded during the first half of the first cycle to another. The former will obtain a lower no-load temperature and higher cooling capacity than the latter. As a whole, COP for IPPTC is higher than that for OPTC.

(3) Turbulence is partly responsible for the bad overall performance of the OPTC, however, it does not form in the IPPTC due to its shorter relaxing time at the hot end.

(4) The streaming, which makes the temperature near the center of the HX higher than the interior at the same cross section, is verified.

## References

- de Boer, P.C.T., 2000. Optimization of the orifice pulse tube. *Cryogenics*, **40**(11):701-711. [doi:10.1016/S0011-2275(01)00003-0]
- de Waele, A.T.A.M., Steijaert, P.P., Koning, J.J., 1998. Thermodynamical aspects of pulse tube II. *Cryogenics*, **38**(3):329-335. [doi:10.1016/S0011-2275(97)00164-1]
- Gao, J.L., Matsubara, Y., 1996. An Inter-phasing Pulse Tube Refrigerator for High Refrigeration Efficiency. Proceedings of ICEC16/ICMC, Kitakyushu, p.295-298.
- Gardner, D.L., Swift, G.W., 1997. Use of inertance in orifice pulse tube refrigerators. *Cryogenics*, **37**(2):117-121. [doi:10.1016/S0011-2275(96)00107-5]
- Kaiser, G., Brehm, H., Thürk, M., Seidel, P., 1996. Thermodynamic analysis of an ideal four-valve pulse tube refrigerator. *Cryogenics*, **36**(7):527-533. [doi:10.1016/0011-2275(96)00017-3]
- Mikulin, E.I., Tarasov, A.A., Shkrebyonock, M.P., 1985. Low temperature pulse tube. *Advances in Cryogenic Engineering*, **31**:49-51.
- Olson, J.R., Swift, G.W., 1997. Acoustic streaming in pulse tube refrigerators: tapered pulse tube. *Cryogenics*, **37**(12):769-776. [doi:10.1016/S0011-2275(97)00037-4]
- Tanida, K., Hiresaki, Y., Matsubara, Y., 1997. Two-stage Inter-phasing Pulse-tube Cooler. Proceedings of the 5th Japanese-Sino Joint Seminar on Cryocooler and its Applications. Osata, Japan, p.72-77.
- Wang, C., Thummes, G., Heiden, C., 1998a. Control of DC gas flow in a single-stage double-inlet pulse tube cooler. *Cryogenics*, **38**(8):843-847. [doi:10.1016/S0011-2275(98)00070-8]
- Wang, C., Thummes, G., Heiden, C., 1998b. Effects of DC gas flow on performance of two-stage 4 K pulse tube coolers. *Cryogenics*, **38**(6):689-695. [doi:10.1016/S0011-2275(98)00044-7]
- Zhang, X.B., Qiu, L.M., 2005. Theoretical analysis on an inner-phasing pulse tube cooler. *Cryogenic Engineering*, **6**:13-16 (in Chinese).
- Zhang, X.B., Qiu, L.M., Gan, Z.H., 2007. CFD simulation on a single orifice pulse tube cooler. *Cryogenics*, **47**(5-6):315-321. [doi:10.1016/j.cryogenics.2007.03.005]
- Zhu, S.W., Wu, P.Y., Chen, Z.Q., 1990. A Single Stage Double-inlet Pulse Tube Refrigerator Capable of Reaching 42 K. Proceedings of 13th ICEC, Beijing, p.567-572.